INT. J. REMOTE SENSING, 2000, VOL. 21, NO. 4, 791–797

Evapotranspiration estimates using NOAA AVHRR imagery in the Pampa region of Argentina

C. M. DI BELLA†, C. M. REBELLA† and J. M. PARUELO‡

†Instituto de Clima y Agua, CIRN–Instituto Nacional de Tecnología Agropecuaria (INTA), Los Reseros y Las Cabañas s/n, Castelar (1712), Buenos Aires, Argentina

‡Departamento de Ecología (IFEVA), Facultad de Agronomía, Universidad de Buenos Aires, Avenida San Martín 4453 (1417), Buenos Aires, Argentina

(*Received 29 June 1998; in final form 19 July 1999*)

Abstract. We used multiple regression analysis to relate evapotranspiration (ET), computed from a water balance technique, to both thermal infrared and normalized difference vegetation index data obtained from the Advanced Very High Resolution Radiometer (AVHRR) sensor on board on the National Oceanic and Atmospheric Administration (NOAA) satellite. This approach, based on only remotely sensed data, provided a reliable estimate of ET over the Pampas, the main agricultural region of Argentina. The relationship between spectral data and ET was more sensitive to the dates than to the sites used to generate the models.

1. Introduction

Evapotranspiration (ET) is a key variable in the calculation of soil water balance, the detection of water stress or the modelling of crop yield (Thunnissen and Nieuwnhuis 1989, Brisson *et al.* 1992). Remotely sensed thermal infrared data have been widely used to estimate ET (e.g. Jackson *et al.* 1983, Caselles *et al.* 1992, Brasa Ramos *et al.* 1996). Estimates of ET have often been derived from the difference between surface and air temperatures (T_s and T_a, respectively) near midday (Seguin and Itier 1983, Vidal and Perrier 1989):

$$ET - R_n = A - B(T_s - T_a) \quad (1)$$

where ET represents the daily evapotranspiration, R_n is the daily net radiation, T_s is the surface temperature calculated from NOAA-AVHRR sensors, T_a is the maximum air temperature and A and B are empirical coefficients. This relationship between ET and crop temperature is derived from the energy balance equation (Jackson *et al.* 1977):

$$R_n = G + H + LE (\mathrm{W\,m^{-2}}) \quad (2)$$

where G is the flux of heat into the soil, H the sensible heat flux from the surface to the atmosphere and LE the latent heat flux. In expression (2), LE corresponds to the amount of water evaporated per unit area (ET) expressed in energy units. Under close canopies, G is small and can be neglected. $T_s - T_a$ in equation (1) becomes then a measure of H. The use of $T_s - T_a$ to estimate ET depends on the availability

International Journal of Remote Sensing
ISSN 0143-1161 print/ISSN 1366-5901 online
http://www.tandf.co.uk/journals/tf/01431161.html

of air temperature data recorded in meteorological stations. A low density of meteorological stations may preclude accurate estimation of the spatial variability of T_a over large areas (Seguin *et al.* 1994).

Several studies have analysed the relationship between ET flux and Normalized Difference Vegetation Index (NDVI) surface temperature information generated from sensors on board meteorological satellites. NDVI data provide a reliable estimate of PAR interception, a variable closely related to biophysical rates such as primary production and ET (e.g. Tucker and Sellers 1986, Box *et al.* 1989, Quattrochi and Pelletier 1991, Paruelo *et al.* 1997). Surface temperature data derived from sensors on board satellites incorporate the effects of topography, surface water and wind, which directly or indirectly modify the ET flux (Kerdiles *et al.* 1996).

In this letter we have calibrated and tested the predictive power of models based on NDVI and surface temperature data derived from NOAA-AVHRR sensors to estimate ET. Taking advantage of the large spatial coverage and the high temporal resolution of meteorological data, our objective was to bridge the gap between local and regional estimates of ET in the Argentine Pampas.

2. Methodology

From July 1982 to January 1983, the Argentine Pampas were affected by a severe drought. We selected six agricultural sites on the northeast portion of the Pampas: Concepción del Uruguay (32°28′S; 58°19′W), Rafaela (31°10′S; 61°33′W), Pergamino (33°55′S; 60°33′W), San Pedro (33°40′S; 59°40′W), Laboulaye (34°7′S; 63°21′W) and Gualeguaychú (33°00′S; 58°37′W). Based on the relationship between the precipitation from July 1982 to January 1983 (PPT) and the mean annual precipitation for a 30-year period (MAP), the rank of drought severity (PPT/MAS) was: Laboulaye (1.11), C. Del Uruguay (0.94), Rafaela (0.79), San Pedro (0.78), Pergamino (0.74) and Gualeguaychú (0.63).

We computed the monthly actual ET for each site using a water balance approach (Thornthwaite and Mather 1957). ET was equal to the potential evapotranspiration (ETP) when the monthly rainfall (PP) exceeded the ETP. If the ETP was greater than the PP, ET was equal to the sum of the rainfall and soil water storage change (ΔW). Meteorological data (precipitation and temperature) were derived from weather stations located within the study sites. We assumed a total soil water storage capacity of 300 mm and an initial soil water content of 300 mm for all the sites.

The estimates of ET were related to both T_s and NDVI values derived from remotely sensed data using multiple regression analysis. Channel 4 (10.3–11.3 μm) brightness temperature data from NOAA-AVHRR sensors were atmospherically corrected using the 'split-window' method (Sobrino *et al.* 1991, 1993) to obtain the corrected temperature (T_c). Monthly T_s values were calculated by averaging T_c for a window of 3×3 pixels centred in each meteorological station. For the same windows and dates, we extracted the monthly composite values of NDVI (table 1).

To evaluate the dependence of the relationship between ET and the spectral data on the sites used, we removed one site from the dataset and we recalculated the regression model. We repeated this procedure for every site. We then repeated the same procedure to evaluate the dependence of the relationship on the dates used. The sites and dates removed were used to generate an independent dataset to test the models. We evaluated the predictive power of the models by using the correlation coefficient, the slope and the *y*-intercept of the relationship between observed and predicted values of ET.

Table 1. Monthly values of rainfall (mm), actual evapotranspiration (*ET*), surface temperature (T_s), normalized difference vegetation index (NDVI) and maximum air temperature (T_a) for the period July 1982–January 1983 for the selected sites.

Study area	Month/year	Rainfall (mm)	*ET* (mm)	T_s (°C)	NDVI	T_a (°C)
Concepción del Uruguay	July 1982	40.30	23.60	16.3	0.30	16.46
Concepción del Uruguay	August 1982	3.00	42.63	19.4	0.38	19.37
Concepción del Uruguay	September 1982	68.60	70.16	24.7	0.50	22.26
Concepción del Uruguay	October 1982	72.20	103.68	23.4	0.57	23.89
Concepción del Uruguay	November 1982	79.70	115.62	26.8	0.52	25.76
Concepción del Uruguay	December 1982	37.10	104.62	32.2	0.50	31.17
Concepción del Uruguay	January 1983	129.00	143.05	49	0.30	32.31
Rafaela	July 1982	7.00	24.58	17.7	0.33	16.94
Rafaela	August 1982	5.30	41.57	18.6	0.39	20.51
Rafaela	September 1982	141.40	77.00	26.6	0.43	22.56
Rafaela	October 1982	27.90	89.91	24.5	0.50	24.78
Rafaela	November 1982	69.70	108.55	34.3	0.46	27.99
Rafaela	December 1982	79.50	116.21	34.6	0.47	30.47
Rafaela	January 1983	150.40	156.11	36.7	0.50	32.28
Pergamino	July 1982	21.70	23.99	17	0.23	14.96
Pergamino	August 1982	0.00	24.68	20.3	0.30	18.54
Pergamino	September 1982	155.20	70.20	21.3	0.46	20.01
Pergamino	October 1982	82.90	105.31	25.7	0.56	22.79
Pergamino	November 1982	112.40	109.60	23.2	0.50	24.25
Pergamino	December 1982	18.80	101.15	56.7	0.44	30.70
Pergamino	January 1983	40.90	83.83	38.2	0.36	32.42
San Pedro	July 1982	71.30	20.50	15.5	0.33	15.01
San Pedro	August 1982	7.50	40.54	17.8	0.34	18.13
San Pedro	September 1982	140.70	67.90	21.8	0.44	20.32
San Pedro	October 1982	99.50	110.59	23.4	0.48	22.98
San Pedro	November 1982	83.30	114.00	29.5	0.46	24.49
San Pedro	December 1982	30.90	120.92	25.8	0.50	30.46
San Pedro	January 1983	79.30	116.94	28.4	0.39	31.44
Laboulaye	July 1982	12.80	21.14	17.9	0.26	15.24
Laboulaye	August 1982	0.00	17.76	19	0.26	18.48
Laboulaye	September 1982	62.50	68.20	18.6	0.43	20.86
Laboulaye	October 1982	32.60	53.48	22.6	0.51	24.37
Laboulaye	November 1982	94.20	102.16	25	0.38	26.00
Laboulaye	December 1982	84.80	95.09	35.5	0.42	30.43
Laboulaye	January 1983	251.10	154.20	30.9	0.54	29.73
Gualeguaychú	July 1982	28.20	24.80	17.5	0.32	16.57
Gualeguaychú	August 1982	25.00	41.53	19.8	0.33	19.44
Gualeguaychú	September 1982	134.90	50.30	23.1	0.41	21.88
Gualeguaychú	October 1982	58.40	104.37	24	0.50	23.61
Gualeguaychú	November 1982	64.90	107.24	28.1	0.47	25.50
Gualeguaychú	December 1982	10.50	90.85	45.2	0.43	31.80
Gualeguaychú	January 1983	77.30	108.71	31.4	0.40	33.03

3. Results and discussion

Most remotely sensed estimates of ET incorporate some sort of ground information (that is, T_a). For large areas of the world in general and for the Pampas in particular the density of meteorological stations is low. An empirical alternative based solely on remotely sensed information will improve significantly the assessment of the water balance over these areas. We found a significant relationship between temperature and NDVI satellite-derived data and ET for the Argentine Pampas ($r^2 = 0.7535$; $n = 41$; $p < 0.0001$):

$$ET = -88.3439 + 1.77636 T_s + 286.406 \mathrm{NDVI}$$

Where ET is in mm and where T_s is in °C, the percentage variance in ET caused by T_s and NDVI data was similar to that obtained by other authors using NDVI, T_s and T_a (Kerr *et al.* 1989, Smith *et al.* 1990, Seguin *et al.* 1994).

The relationship between ET and remotely sensed data was quite stable (table 2). The sites included in the analysis encompassed the full range of land cover types found in the Pampas, from natural grasslands (Gualeguaychú) to intensive agriculture (Pergamino). However, differences in land cover among sites have almost no effect on the relationship between ET and NDVI-T_s (table 2). When we evaluated the temporal effect, the extraction of the July and August data reduced the r^2 values but it generated minor changes in the coefficients of the models (table 3). These months showed the lowest values of ET.

ET values calculated from the water balance method and derived from remotely sensed data were highly correlated ($r = 0.79$, $p < 0.0001$, for the dataset with sites removed and $r = 0.70$, $p < 0.001$, for the dataset with dates removed). However, the slopes of the lines fitted to the observed and estimated ET values differed significantly ($p < 0.01$) from 1 and the y-intercepts differed from zero for both datasets, indicating that the NDVI–T_s model underestimated the highest values of ET (figures 1 and 2). Several factors may account for this lack of fit. The saturation of the NDVI–ET relationship at this level of ET may be one of these factors. Uncertainties associated with the estimates of ET derived from the water balance may be another. The monthly resolution of the method may not be detailed enough to track water losses. The size and distribution of the precipitation events are critical information in

Table 2. Regression coefficients, slopes and y-intercepts resulting from removing one site from the dataset and recalculating the regression model.

Site removed	r^2	y-intercept	NDVI slope	T_s slope
Concepción del Uruguay	0.75	− 90.90	304.63	1.65
Gualeguaychú	0.74	− 84.44	242.18	2.41
Laboulaye	0.74	− 85.51	256.91	2.17
Pergamino	0.79	− 98.00	232.89	3.13
Rafaela	0.70	− 76.56	243.21	2.07
San Pedro	0.74	− 81.85	240.42	2.22

Table 3. Regression coefficients, slopes and y-intercepts resulting from removing one month from the dataset and recalculating the regression model.

Month removed	r^2	y-intercept	NDVI slope	T_s slope
July	0.60	− 77.59	243.39	2.14
August	0.67	− 75.05	238.57	2.14
September	0.75	− 85.42	263.65	2.15
October	0.76	− 91.90	279.63	2.13
November	0.74	− 84.43	242.75	2.28
December	0.85	− 107.10	221.33	3.76
January	0.79	− 81.46	282.76	1.40

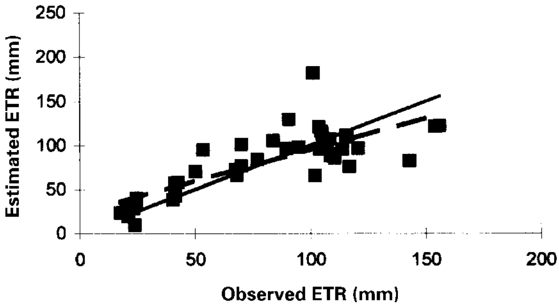

Figure 1. Relationship between *ET* calculated from meteorological data (observed) and estimated from remotely sensed data. The solid line corresponds to the 1:1 relation and the dashed line to the regression equation. The independent data were generated by removing one site from the dataset used to generate the model. The procedure was repeated for every site. $y = 0.7188x + 23.112$, $r = 0.79$.

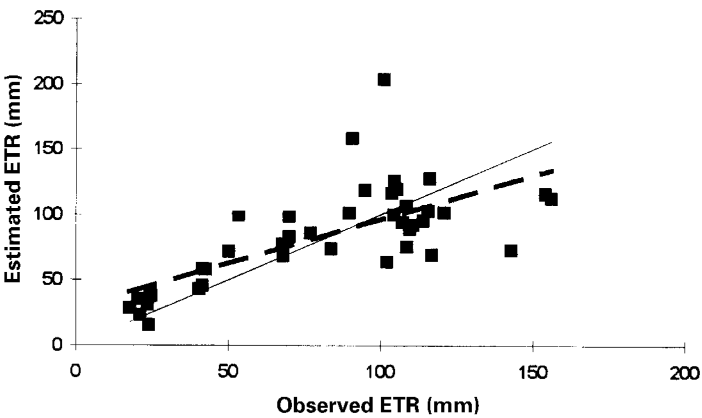

Figure 2. Relationship between *ET* calculated from meteorological data (observed) and estimated from remotely sensed data. The solid line corresponds to the 1:1 relation and the dashed line to the regression equation. The independent data were generated by removing one date from the dataset used to generate the model. The procedure was repeated for every date. $y = 0.6766x + 28.551$, $r = 0.70$.

calculating the water balance (Paruelo and Sala 1995). Unfortunately daily meteorological data were not available for the period and sites considered.

Despite the differences between observed and predicted values for high ET conditions, the combination of NDVI and atmospherically corrected thermal channel radiance (T4) seems to be a good approach for estimating ET at a regional scale. This approach may be an important tool for solving the gap between local and regional monitoring of drought. The estimates of ET derived from point data interpolation differed considerably from those calculated from remotely sensed data (figure 3). For example, ET estimates for areas such as northwest Pergamino (Pe) derived from point data interpolation may differ by more than 30 mm from those calculated from remotely sensed data, providing a completely different view of the water balance of the area.

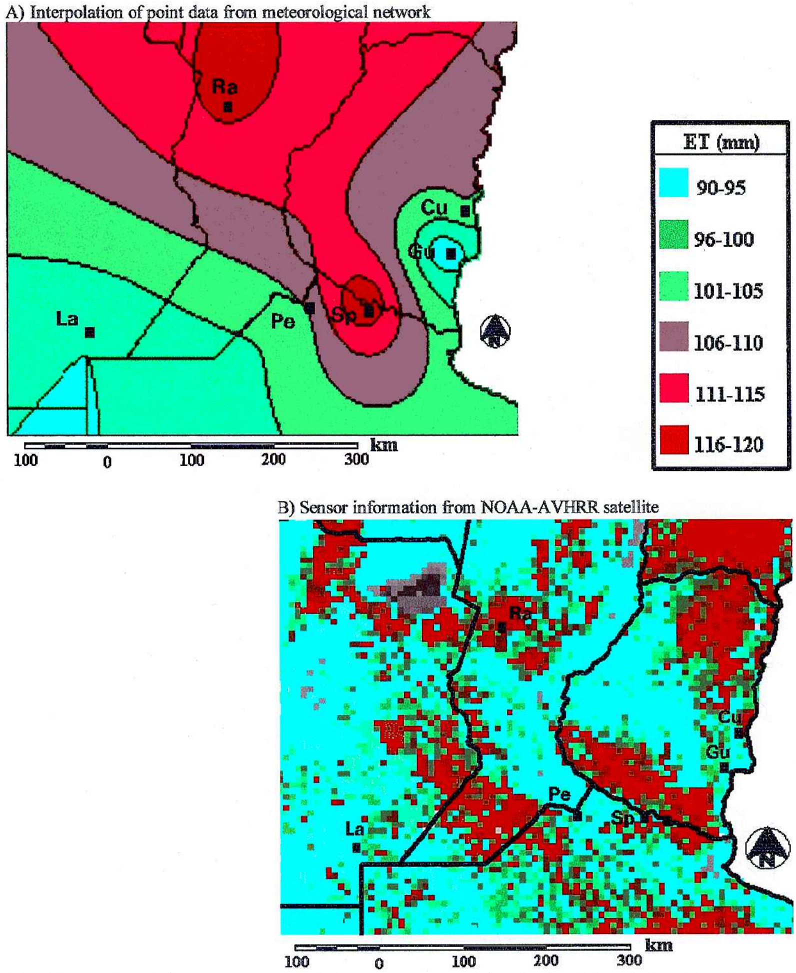

Figure 3. *ET* estimates from interpolation (*a*) of point data and (*b*) from sensor data for the month of December 1982.

Acknowledgments

We thank Mr Patricio Oricchio for the gathering of data and Dr B. Seguin (INRA, Unité de Bioclimatologie, Avignon, France) for his valuable comments. This research was conducted under the project 'Hydrological Determinants of Agriculture in Latin America: Remote Sensing and Numerical Simulation'. Contract STD3/HAG/TS3*CT-0239 was sponsored by the European Union. J. M. P. was supported by the Universidad de Buenos Aires, Fundación Antorchas and CONICET.

References

Box, E. O., Holben, B. N., and Kalb, V., 1989, Accuracy of the AVHRR vegetation index as a predictor of biomass, primary productivity and net CO_2 flux. *Vegetatio*, **80**, 71–89.

Brasa Ramos, A., De Santolalla, F. M., and Caselles, V., 1996, Maximum and actual evapotranspiration for barley (*Hordeum vulgare* L.) through NOAA satellite images in Castilla-La Mancha, Spain. *Journal of Agricultural Engineering Research*, **63**, 283–294.

Brisson, N., Seguin, B., and Bertuzzi, P., 1992, Agrometeorological soil water balance for crop simulation models. *Agricultural and Forest Meteorology*, **59**, 267–287.

Caselles, V., Delegido, J., Sobrino, J. A., and Hurtado, E., 1992, Evaluation of the maximum evapotranspiration over the La Mancha Region, Spain, using NOAA AVHRR data. *International Journal of Remote Sensing*, **13**, 939–946.

Jackson, R. D., Hatfield, J. L., Reginato, R. J., Idso, S. B., and Pinter Jr., P. J., 1983, Estimation of daily evapotranspiration from one time-of-day measurements. *Agricultural Water Management*, **7**, 351–362.

Jackson, R. D., Reginato, J. L., and Idso, S. B., 1977, Wheat canopy temperature: a practical tool for evaluating water requirements. *Water Resources Research*, **13**, 651–656.

Kerdiles, H., grondona, M., Rodriguez, R., and Seguin, B., 1996, Forest mapping using NOAA-AVHRR data in the Pampean Region, Argentina. *Agricultural and Forest Meteorology*, **79**, 157–182.

Kerr, Y. H., Imbernon, J., Dedieu, G., Hautecouer, O., Lagouarde, J. P., and Seguin, B., 1989, NOAA-AVHRR and its uses for rainfall and evapotranspiration monitoring. *International Journal of Remote Sensing*, **10**, 847–854.

Paruelo, J. M., and Sala, O. E., 1995, Water losses in the Patagonian steppe: a modelling approach. *Ecology*, **76**, 510–520.

Paruelo, J. M., Epstein, H. E., Lauenroth, W. K., and Burke, I. C., 1997, ANPP estimates from NDVI for the Central Grassland Region of the U.S. *Ecology*, **78**, 953–958.

Quattrochi, D. A., and Pelletier, R. E., 1991, 3. Remote Sensing for Analysis of Landscapes. *Ecological Studies*, **82**, 51–76.

Seguin, B., Couralt, D., and Guerif, M., 1994, Surface temperature and evapotranspiration: Application of local scale methods to regional scales using satellite data. *Remote Sensing of Environment*, **49**, 287–295.

Seguin, B., and Itier, B., 1983, Using midday surface temperature to estimate daily evaporation from satellite thermal IR data. *International Journal of Remote Sensing*, **4**, 371–383.

Smith, R. C. G., and Choudhury, B. J., 1990, Relationship of multispectral satellite data to land surface evaporation from the Australian continent. *International Journal of Remote Sensing*, **11**, 2069–2088.

Sobrino, J. A., Caselles, V., and Coll, C., 1993, Theoretical split-window algorithms for determining the actual surface temperature. *Il Nuovo Cimento*, **16**, 219–236.

Sobrino, J. A., Coll, C., and Caselles, V., 1991, Atmospheric correction for land surface temperature using NOAA-11 AVHRR Channels 4 and 5. *Remote Sensing of Environment*, **38**, 19–34.

Thornthwaite, C. W., and Mather, J. R., 1957, Instructions and tables for computing potential evapotranspiration and the water balance. In *Publications in Climatology*, Vol. 10, no. 3 (Drexel Institute of Technology: Laboratory of Climatology), p. 308.

Thunnisen, H. A. M., and Nieuwenhuis, G. J. A., 1989, An application of remote sensing and soil water balance simulation models to determine the effect of groundwater extraction on crop evapotranspiration. *Agricultural Water Management*, **15**, 315–332.

Tucker, C. J., and Sellers, P. J., 1986, Satellite remote sensing of primary production. *International Journal of Remote Sensing*, **7**, 1395–1416.

Vidal, A., and Perrier, A., 1989, Analysis of a simplified relation for estimating daily evapotranspiration from satellite thermal IR data. *International Journal of Remote Sensing*, **10**, 1327–1337.